which have, respectively, uniformly convergent and asymptotically convergent expansions

$$F(\alpha,\beta;x)=1+\frac{\alpha}{\beta}\left(\frac{x}{1!}\right)+\frac{\alpha(\alpha+1)}{\beta(\beta+1)}\left(\frac{x^2}{2!}\right)+\cdots,$$
$$G(\alpha,\beta;x)=\frac{(\beta-1)!}{(\beta-1-\alpha)!}(-x)^{-\alpha}\left\{1-\alpha(\alpha-\beta+1)\left(\frac{1}{1!x}\right)+\alpha(\alpha+1)(\alpha-\beta+1)(\alpha-\beta+2)\left(\frac{1}{2!x^2}\right)+\cdots\right\}. \tag{A5}$$

Also, E or η is determined by the continuity of $(d/dr)\ln\Psi_E(r)$ at $r=R$ and N is fixed on the basis of the normalization condition: $\int[\Psi_E(r)]^2 4\pi r^2 dr=1$.

We now confine ourselves to the case of low-Z nuclei, where $R/a\ll 1$. Here

$$\eta\cong 1; \qquad \cong\tfrac{3}{2}(R/a)^{1/2};$$
$$G(-\eta+1,2;2r/\eta a)\cong G(0,2;2r/\eta a)=1: \quad r\geqq R;\ N\cong 1. \tag{A6}$$

Substitution of Eqs. (A6) and (A3) into Eq. (A2) then gives

$$C(N_a)\cong\left[\exp\left(-\frac{2R}{a}\right)\right]\left\{\frac{3}{R^3}\int_0^R \frac{F(\frac{1}{2}(\frac{3}{2}-\epsilon),\frac{3}{2};(R/a)^{1/2}(r^2/a^2))}{F(\frac{1}{2}(\frac{3}{2}-\epsilon),\frac{3}{2};(R/a)^{1/2})}\exp\left[-\frac{1}{2}\left(\frac{R}{a}\right)^{1/2}\left(\frac{r^2-R^2}{R^2}\right)\right]r^2dr\right\}^2$$
$$=\begin{cases}0.965: & \mathrm{He}^3(Z=2)\\ 0.928: & \mathrm{Li}^6(Z=3)\\ 0.885: & \mathrm{C}^{12}(Z=6)\end{cases}. \tag{A7}$$

PHYSICAL REVIEW VOLUME 140, NUMBER 3B 8 NOVEMBER 1965

Proton Total Reaction Cross Sections at 16.4 MeV†

ROBERT E. POLLOCK AND G. SCHRANK*
Palmer Physical Laboratory, Princeton University, Princeton, New Jersey
(Received 28 May 1965)

Total reaction cross sections for protons of a laboratory energy of 16.4 MeV at the center of foil targets of C, Mg, Al, Ni, Cu, and Pb have been measured by a beam attenuation method. The technique differs from other measurements with intermediate energy protons in that a double-focusing magnetic spectrometer is contained within the scintillation counter telescope which precedes the target. The magnet selects a beam free from slit-scattered protons, with a precisely determined momentum, while the focusing compensates for the beam divergence in the first detector so that all detectors see comparable counting rates. Solid-state circuitry with controlled recovery characteristics was developed to permit instantaneous rates in excess of 10^6 protons/sec and to circumvent the problem of a low duty cycle. The measurements require several major corrections, and continuing effort to improve the evaluation of these corrections since this measurement was first described has led to the following values for reaction cross sections:

Target	C	Mg	Al	Ni	Cu	Pb
σ_R(mb)	368	712	701	898	955	1330
Standard deviation	30	56	34	53	64	180

Total reaction cross sections have been predicted by optical-model analyses of proton elastic scattering at this energy with a variety of optical potentials. The measured values for Ni and Cu lie somewhat lower than the predictions of the optical model, while the values for Pb and C are higher than the predictions.

I. INTRODUCTION

TOTAL reaction cross sections determined by experiment can restrict the choice of scattering potential used to describe the nucleon-nucleus interaction. Early in the development of a suitable optical potential, the need for realistic reaction cross sections led to diffuse-edged potentials much as realistic polarizations required the added spin-orbit interactions. With the many-parameter potentials now in common use, it is misleading to speak of one experiment as determining one or another parameter since all are effective to varying extents. A helpful description of the way in

† This work was supported in part by the U. S. Atomic Energy Commission and the Higgins Scientific Trust Fund.
* Present address: Department of Physics, University of California, Santa Barbara, California.

which experiments fix the potential is obtained by considering a parameter space in which one dimension is allotted to each potential parameter. Any experiment determines a region in parameter space with uncertain boundaries set by the experimental error. In some instances the elastic scattering data alone may give a region so limited that one can say the parameters are unambiguously determined. In other cases[1] an elongated region specified by elastic scattering may be intersected by the region determined by a reaction cross section experiment which then serves to limit the range of potential parameters. When reliable experiments determine regions having no overlap, the need for a potential of modified form is indicated. Thus, while it may be naive to expect reaction cross section experiments to compete, except in special cases, with the accuracy and high information content of angular distributions as a method of fixing the optical potential, interest in these measurements will continue because discovery of significant disagreements of the latter type must lead to further elaboration and refinement of the optical potential, and perhaps ultimately help delineate the validity limits of the model.

The present work was undertaken to complement the elastic scattering[2–4] and polarization[5,6] data in this energy region which had been a testing ground in several optical-model investigations.[7–10] When the work began in 1960, no reaction cross section experiments at energies this low had been reported so the accuracy limits were unknown and considerable effort was devoted to an exploration of the limitations of the method. This aspect of the experiment has been reported in detail elsewhere.[11,12] More recently, reaction cross section measurements have become increasingly common.

Measurement techniques for total reaction cross sections fall into four classes. For neutrons, or for charged particles of very high energies, the total cross section (reactions plus elastic scattering) may be measured by a "good" geometry attenuation experiment, followed by subtraction of the total elastic scattering given by integration over measured elastic angular distributions. Very thick targets may be used to give large fractional attenuations so that the total cross sections are determined to high accuracy and the limitation in the accuracy of the total reaction cross section is set by the elastic subtraction.

For charged particles at lower energies, an attenuation measurement with "bad" geometry must be used to avoid large subtractions from Coulomb scattering at forward angles. The charged-particle elastic scattering at large angles is measurable with high precision so that the accuracy is not limited by the subtraction. However, the large angle subtended by the detector in "bad" geometry leads to a sizable fraction of the forward inelastic scattering not being recorded as attenuation events, the fraction being determined by the angle and energy resolution of the counter following the target. Moreover, the target thickness is limited by the permissable energy loss so that the fractional attenuation is small and many events must be processed to attain moderate statistical accuracy in the attenuation measurement. While measurements by Gooding[13] and Meyer *et al.*[14] showed that the technique of Cassels and Lawson[15] could be extended to lower energies, attenuation measurements for low-energy charged particles have become common only more recently as techniques for detection and analysis at high counting rates have improved. When a discriminator is used with the final counter to restrict the energy interval of the forward inelastic correction, nuclear reactions in this counter which are indistinguishable from forward inelastic scattering from the target will give rise to a large attenuation background which persists when the target is removed and which enhances the difficulty from the small attenuation in the target.

An increase in the incident energy will increase the number of attenuation events in the stopping counter and will have the same effect as adding a target made of the stopping material as thick as the increase in range. Burge[16] has suggested using the energy dependence of the detector attenuation as an alternative measure of reaction cross sections for the limited class of materials which can be used as detectors.

The final class of measurements of total reaction cross sections is that in which the partial cross sections for all possible reactions are separately determined and summed. The summation method is feasible only at energies where only a few reaction channels are open. The accuracy limit is usually set in this method by difficulties in determining absolute neutron cross sections.

In the present work each of the last three methods was applied to a determination of the reaction cross section for carbon; in this way a confirmation of the accuracy of the attenuation method used on the other targets can be obtained as well as a comparison of the

[1] M. A. Melkanoff, J. S. Nodvik, and D. S. Saxon, in *Proceedings of the Rutherford Jubilee International Conference, Manchester, 1961* (Academic Press, Inc., New York, 1961), p. 411.
[2] I. E. Dayton and G. Schrank, Phys. Rev. **101**, 1358 (1956).
[3] W. W. Daehnick and R. Sherr, Phys. Rev. **133**, B934 (1964).
[4] G. Schrank and R. E. Pollock, Phys. Rev. **132**, 2200 (1963).
[5] K. W. Brockman, Phys. Rev. **110**, 163 (1958).
[6] W. A. Blanpied, Phys. Rev. **113**, 1099 (1959).
[7] M. A. Melkanoff, J. S. Nodvik, D. S. Saxon, and R. D. Woods, Phys. Rev. **106**, 793 (1957).
[8] A. E. Glassgold and P. J. Kellogg, Phys. Rev. **107**, 1372 (1957).
[9] E. J. Burge, R. A. Giles, and P. E. Hodgson, Proc. Phys. Soc. (London) **81**, 832 (1963).
[10] F. G. Perey, Phys. Rev. **131**, 745 (1963).
[11] R. E. Pollock and G. Schrank, Bull. Am. Phys. Soc. **7**, 72 (1962).
[12] R. E. Pollock, Ph.D. thesis, Princeton University, 1962 (unpublished).
[13] T. J. Gooding, Nucl. Phys. **12**, 241 (1959).
[14] V. Meyer, R. M. Eisberg, and R. F. Carlson, Phys. Rev. **117**, 1334 (1960).
[15] J. M. Cassels and J. D. Lawson, Proc. Phys. Soc. (London) **A67**, 125 (1954).
[16] E. J. Burge, Nucl. Phys. **13**, 511 (1959).

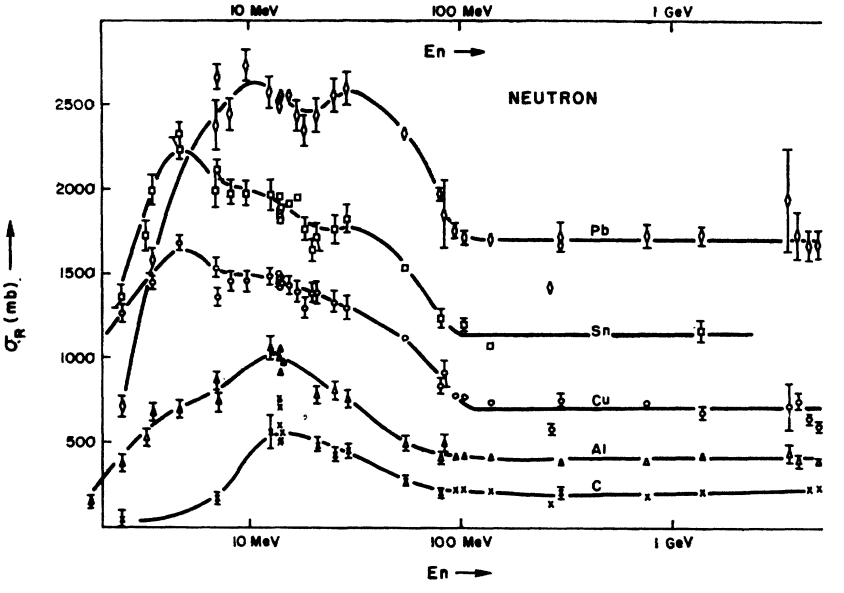

FIG. 1. Neutron total reaction cross sections for five typical nuclei plotted against the logarithm of the neutron energy. Reference key in Table I. The lines are drawn by eye to connect the points.

relative usefulness of the three methods which are possible in this energy region.

To illustrate the systematic behavior with energy and mass number of total reaction cross sections for neutrons and protons, Figs. 1 and 2 show a compilation, reasonably complete up to the summer of 1962, for five nuclei most commonly studied (C, Al, Cu, Sn, and Pb, with substitution of neighboring elements where necessary). Table I provides a key to the literature for these figures. The energy scale is logarithmic spanning four orders of magnitude with the one experiment at 22 GeV displaced downward in energy to remain on scale. The lines are drawn by eye to connect related points.

Certain general features of the systematic behavior of the total reaction cross section may be discerned in these two figures. Above 100 MeV the data are consistent with complete energy independence. A weighted average of all the high-energy data is shown in Fig. 3, plotted against $A^{2/3}$ and is fitted very well by a straight line with negative intercept. The slope gives a value of the nuclear radius parameter $r_0=1.26\pm0.01$ F and the negative intercept could be explained[17] by a mean free path λ in nuclear matter of 1.8 ± 0.3 F. Both these parameters are the same for protons as for neutrons within the stated errors. The radius r_0 determined in this manner from the high-energy data is consistent with radii chosen for many optical analyses at lower

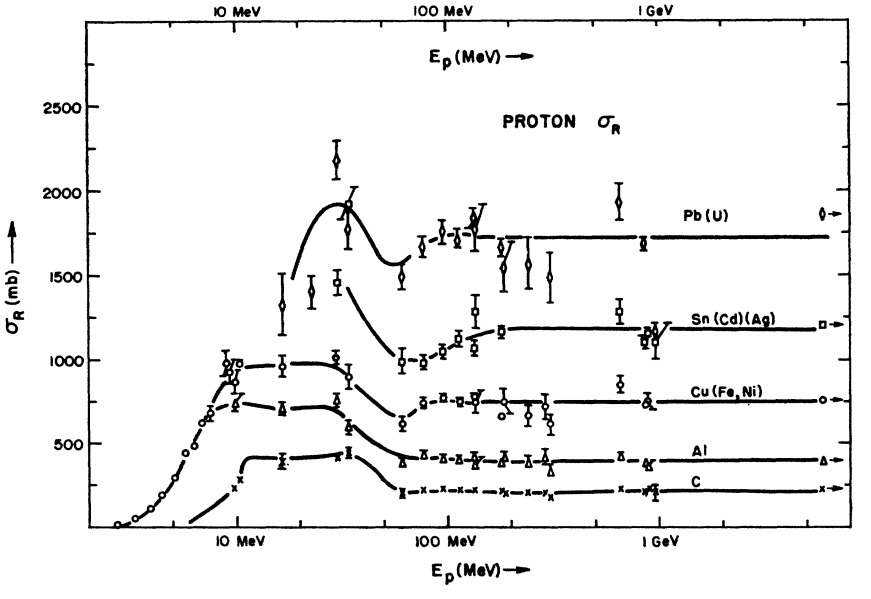

FIG. 2. Proton total reaction cross sections for five typical nuclei plotted against the logarithm of the proton energy. Reference key in Table I. The lines are drawn by eye to connect the points.

[17] H. G. De Carvalho, Phys. Rev. 96, 407 (1954).

TABLE I. Reference key for figures. The data shown in Figs. 1 and 2 come from many sources. This key relating energy to references will assist in the location of particular experiments.

Neutron energy (MeV)	References	Proton energy (MeV)	References
1.0, 1.77, 2.5, 3.25, 7	a	Low	b
3.5, 4.7, 7.1, 12.7, 14, 14.1	c	7.5	d
8.2, 9.8, 15.5, 17.0, 18.5, 20.0	e	9	f
14	g, h, i	9.3	j
14.2	k	9.85	l, m
21, 25.5, 29.2	n	10.3	o
55, 81, 105, 140	p	16.4	Present work
84	q	22.8	r
95	s	29	t
270	u	34	v
300	w	61	x
765	y	77, 95, 113, 133	z
1.4 GeV	aa	134	bb
3.6	cc	180	dd
4.0	ee	185, 240, 305	ff
4.5, 5.0	gg	290	hh
		657	ii
		860	jj
		895	kk
		950	ll
		24 200	mm

[a] J. R. Beyster, M. Walt, and E. W. Salmi, Phys. Rev. **104**, 1326 (1956).
[b] R. Fox and R. D. Alpert, Phys. Rev. **121**, 1779 (1961).
[c] H. L. Taylor, O. Lonsjo, and T. W. Bonner, Phys. Rev. **100**, 174 (1955).
[d] B. W. Shore, N. S. Wall, and J. W. Irvine, Jr., Phys. Rev. **123**, 276 (1961).
[e] T. W. Bonner and J. C. Slattery, Phys. Rev. **113**, 1088 (1959).
[f] R. F. Carlson, R. M. Eisberg, R. H. Stokes, and T. H. Short, Nucl. Phys. **36**, 511 (1962).
[g] E. R. Graves and R. W. Davis, Phys. Rev. **97**, 1205 (1955).
[h] D. D. Phillips, R. W. Davis, and E. R. Graves, Phys. Rev. **88**, 600 (1952).
[i] N. N. Flerov and V. M. Talyzin, At. Energ. (USSR) **4**, 155 (1956); [English transl.: **4**, 617 (1956)].
[j] G. W. Greenlees and O. N. Jarvis, *Proceedings of the International Conference on Nuclear Structure, 1960*, edited by D. A. Bromley and E. W. Vogt (North-Holland Publishing Company, Amsterdam, 1960), p. 217.
[k] Reference 25.
[l] V. Meyer and N. H. Hintz, Phys. Rev. Letters **5**, 207 (1960).
[m] R. D. Alpert and L. F. Hansen, Phys. Rev. Letters **6**, 13 (1961).
[n] M. H. MacGregor, *Proceedings of the International Conference on the Peaceful Uses of Atomic Energy, Geneva, 1958* (United Nations, Geneva, 1958), Vol. 14, p. 109.
[o] Reference 26.
[p] R. G. P. Voss and R. Wilson, Proc. Phys. Soc. (London), **A236**, 41 (1956).
[q] A. Bratenahl, S. Fernbach, R. H. Hildebrand, C. E. Leith, B. J. Moyer, J. DeJuren, and N. Knable, Phys. Rev. **77**, 597 (1950).
[r] C. B. Fulmer, Phys. Rev. **116**, 418 (1960).
[s] J. DeJuren and N. Knable, Phys. Rev. **77**, 606 (1950).
[t] Reference 21.
[u] J. DeJuren, Phys. Rev. **80**, 27 (1950).
[v] Reference 13.
[w] W. P. Ball, thesis, U.C.R.L. 1938, 1952 (unpublished), reported in Millburn *et al.*, Phys. Rev. **95**, 1268 (1954).
[x] Reference 14.
[y] N. E. Booth, G. W. Hutchinson, and B. Ledley, Proc. Phys. Soc. (London), **A71**, 293 (1958).
[z] R. Goloskie and K. Strauch, Nucl. Phys. **29**, 474 (1962).
[aa] T. Coor, D. A. Hill, W. F. Hornyak, L. W. Smith, and G. Snow, Phys. Rev. **98**, 1369 (1955).
[bb] Reference 15.
[cc] P. H. Barrett, Phys. Rev. **114**, 1374 (1959).
[dd] A. Johansson, U. Svanberg, and O. Sundberg, Arkiv Fysik **19**, 527 (1961).
[ee] M. S. Sinha and N. C. Das, Phys. Rev. **105**, 1587 (1957).
[ff] A. J. Kirshbaum, thesis, University of California Radiation Laboratory Report No. UCRL-1967, 1952 (unpublished), reported in Millburn *et al.*, Phys. Rev. **95**, 1268 (1954).
[gg] J. H. Atkinson, W. N. Hess, V. Perez-Mendez, and R. W. Wallace, Phys. Rev. Letters **2**, 168 (1959) and Phys. Rev. **123**, 1854 (1961).
[hh] G. P. Millburn, W. Birnbaum, W. E. Crandall, and L. Schecter, Phys. Rev. **95**, 1268 (1954).
[ii] V. I. Moskalev and B. V. Gavrilovskii, Dokl. Akad. Nauk SSSR **110**, 972 (1956) [English transl.: Soviet Phys.—Doklady **1**, 607 (1956)].
[jj] F. F. Chen, C. P. Leavitt, and A. M. Shapiro, Phys. Rev. **99**, 857 (1955).
[kk] N. E. Booth, B. Ledley, D. Walker, and D. H. White, Proc. Phys. Soc. (London) **A70**, 209 (1957).
[ll] W. O. Lock, P. V. March, H. Muirhead, and W. G. V. Rosser, Proc. Roy. Soc. (London) **A230**, 215 (1955).
[mm] A. Ashmore, G. Cocconi, A. N. Diddens, and A. M. Wetherell, Phys. Rev. Letters **5**, 576 (1960).

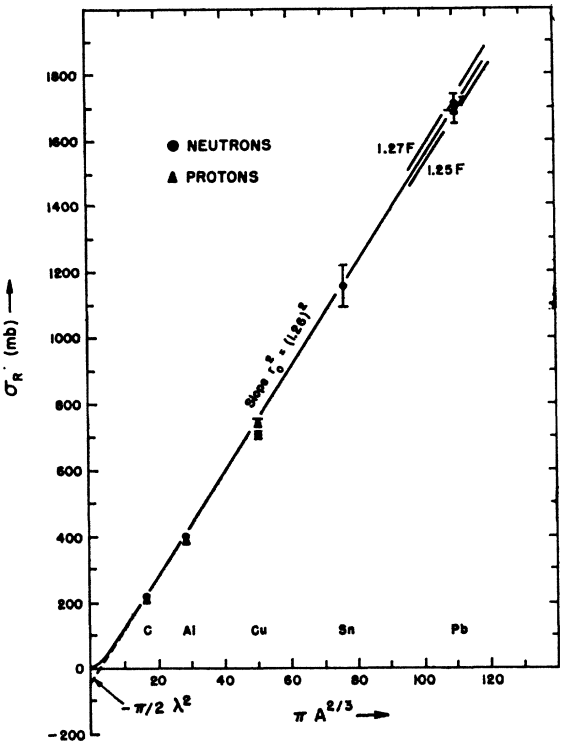

FIG. 3. The average values of reaction cross sections above 150 MeV are plotted against $A^{2/3}$. The solid line represents the best fit with a nuclear radius $r_0=1.26$ F and a mean free path in the interior of 1.8 F.

energies. The mean free path is expected to depend on optical potential parameters[18] and so to vary slightly with energy. The data are not sufficiently precise to follow this point further. An alternative A dependence at high energies has been proposed[19] which is based on the scattering by individual nucleons in the nucleus and the shielding effect caused by close packing. The high-energy average σ_R are also consistent with this interpretation.

Below 100 MeV the increasing neutron wavelength raises the reaction cross sections for neutrons but for protons the Coulomb path distortion has an opposite effect and the proton reaction cross sections are seen to rise less with reduced energy. Oscillation about this gross behavior in the 10–100-MeV region for both protons and neutrons is seen in the figures and indeed is expected from classical diffraction theory[20] at these energies. At still lower energies the cross section falls to a small value as the nucleus becomes increasingly transparent. Except where the Coulomb barrier dominates the behavior for protons on heavy nuclei, the behavior for low energies is seen to vary markedly

[18] F. L. Friedman and V. F. Weisskopf, *Neils Bohr and the Development of Modern Physics* (McGraw-Hill Book Company, New York, 1955), p. 134.
[19] N. R. Steenberg, Nucl. Phys. **35**, 455 (1962).
[20] K. W. McVoy, Bull. Am. Phys. Soc. **9**, 16 (1964).

from one nucleus to another, depending on details of the open reaction channels.

In Fig. 2, the measurements of Makino, Waddell, and Eisberg[21] show that the proton reaction cross section for Ag at 29 MeV ($\sigma_R = 1471 \pm 71$ mb) is rather higher than the other σ_R values for protons on nuclei of this mass might have indicated ($\sigma_R \sim 1200$ mb). The high value is, however, supported by the early high measurement by Gooding[13] of σ_R for protons on Sn at 34 MeV of 1930 ± 100 mb. There would appear to be a solitary distinct maximum in the proton σ_R on the A, E_p plane near this location. More measurements will be needed to explore this apparent anomaly.

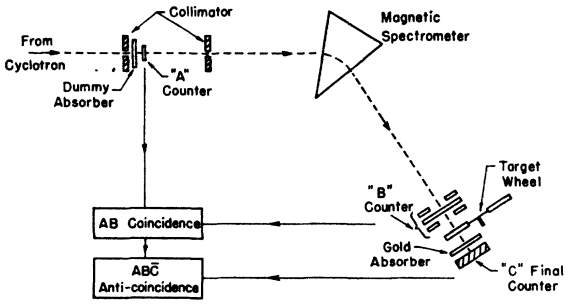

FIG. 4. Schematic diagram of the experimental geometry with the scale of the detector assemblies magnified for clarity.

II. EXPERIMENTAL DESIGN

The attenuation measurement is accomplished by following every proton in a prepared beam as it passes through the target and recording the small fraction of the protons which reacts. This section describes the apparatus which performs this task and then the method used to acquire the attenuation data.

(a) Geometry

Figure 4 is a sketch of the detector arrangement as seen from above, with scale distorted for clarity. The external beam of the Princeton FM cyclotron is directed by steering and focusing magnets onto the $\frac{1}{8}$-in.-diameter aperture of the front collimator. The spectrometer magnet images the collimator at the position of counter B, sweeping from the beam all low-energy protons from up-stream scattering. Counters A and B are sheets of plastic scintillator NE 102, a few thousandths of an inch in thickness, mounted perpendicular both to the proton beam and to the end window of an RCA 6342 A photomultiplier. The mount is a slotted Lucite lightguide with silicone oil coupling, wrapped in aluminum foil. Counter B is itself the exit aperture for the magnet, having additional sheets of scintillator with a hole in the center mounted in the same lightguide. Protons not centered in this counter can thus be identified by the larger pulse height and rejected electronically. A pulse from counter A, followed after the 50-nsec flight time through the magnet by a suitable pulse from B, indicates a proton of known energy incident on the target center. The six-position target wheel is followed by a $1\frac{1}{2}$-in.-diameter button of NE 102 mounted with a short lightpipe on a photomultiplier to form the C counter. Counter B is fixed in position but the target holder and the C counter assembly may be independently withdrawn along the beam line to vary the angles subtended by C at the target and at B.

The beam divergence arising from multiple scattering in counter A throws roughly half the beam outside the spectrometer-magnet acceptance angle. An absorber which can be introduced near A to lower the beam energy by 1 MeV and simulate the target energy loss reduces the magnet transmission by another factor of 2. Without the magnetic focusing, the beam transmission factor from A to B would be much worse. The dispersion of the spectrometer and the intrinsic cyclotron energy spread combine to determine the horizontal beam profile at the magnet exit. Seen on a phosphor screen the beam appears about 1 cm wide and 1 mm high. The aperture of B is large enough to accept the entire beam spot. The size and elongated shape of the beam spot introduce certain complications in the scattering corrections. Considering all the other factors involved, however, the magnet used in this way is definitely advantageous.

(b) Electronics

Figure 5 is a block diagram of the electronic system. The preamplifiers, discriminators, coincidence circuitry, and prescalars were developed for this experiment using low peak current tunnel diodes (GE 1N2939 and 1N2969) and the Philco 2N501 transistor. Care was taken to control recovery times with extensive dc coupling. The differential discriminators of counters A and B reject pileup and uncentered protons, respectively. The integral C discriminator determines the critical energy loss beyond which an event is labeled a reaction. By placing this output in anticoincidence all reaction events are recorded in the scalar labeled $AB\bar{C}$ and all the incident protons in the scalar AB so that the ratio $AB\bar{C}/AB$ is the measured fractional attenuation. The discriminator levels were fixed by the tunnel diode bias and the positioning set by the photomultiplier voltage while monitoring the appropriate gated spectrum.

The coincidence circuits follow the discriminators which have time walks of 20 nsec so the coincidence resolving time is set at ($2\tau = 50$ nsec) and the anticoincidence resolving time at 100 nsec. The coincidence circuit is purposely paralyzed long enough for complete recovery of the anticoincidence circuit. In measuring small attenuations, the operation of the anticoincidence must be absolutely sure to a few parts per million.

[21] M. O. Makino, C. H. Waddell, and R. M. Eisberg, Nucl. Phys. **50**, 145 (1964).

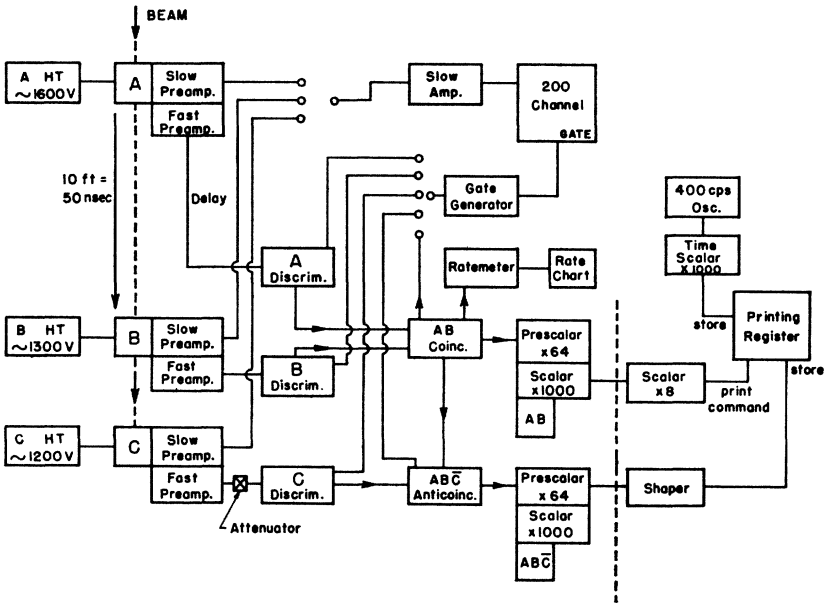

FIG. 5. Block diagram of the electronic system. The fast recovery circuitry was designed for the specific requirements of this experiment.

Since background and accidental rates are negligible these comparatively large resolving times are adequate.

The recovery characteristics of the fast circuitry were investigated with a high-repetition-rate pulser gated in bursts to simulate the cyclotron beam. The waveforms from double or triple pulsing were not indicative of the burst response in all cases. The properties of the commerical microsecond circuitry making up the remainder of the electronic system were not critical to this experiment and will not be described.

(c) Alignment and Testing

Physical alignment was accomplished with fluorescent screens in the early stages, while the final adjustments were made by maximizing the magnet transmission: the ratio AB/A. The spectrometer magnetic field was readjusted from time to time to compensate for slight energy shifts in the cyclotron proper. The very low beam current from the cyclotron was obtained by simply lowering the rf dee voltage to about 1 kV peak-to-peak. All other cyclotron parameters were adjusted for maximum beam to help stability. For this it was found necessary to run a very feeble arc in the ion source.

The spectrum in counter A showed a single peak well separated from the photomultiplier noise so the discriminator setting was straightforward. The spectrum of counter B showed additional peaks for off-center protons which could be identified by changing the spectrometer magnetic field to move the beam spot onto the edges of B. The correct magnetic field and hence the beam energy was easily determined to within 50 keV by minimizing the counting rate in these peaks. Since the setting of the C discriminator determined the cutoff in the inelastic corrections and the size of the attenuation background from reactions in the C scintillator a more elaborate procedure to accomplish this adjustment was adopted. The spectrum of the C counter is shown in Fig. 6. A prominent feature in the low-energy tail arose from inelastic scattering to the first excited state at 4.43 MeV of the C^{12} in the plastic scintillator. The C discriminator was set by gain adjustments to lie in the valley corresponding to 3.3 MeV of energy loss as shown by the arrow. Small changes were made in the discriminator setting to correct for differences in target energy loss as each target was placed in the beam. The beam spot could be moved across C in a horizontal plane to compare response between center and edges. The difference was never worse than about 2%.

The area in the low-energy tail from attenuation events in the scintillator was 0.50%: 5000 ppm at 17 MeV, while the target attenuations were on the order of 500 ppm. The attenuation background greatly lengthens the time required for a given statistical accuracy. By introducing 300 mg/cm^2 of Au between target and counter, the attenuation background could be lowered to 3500 ppm, halving the running time and improving the situation for scattering corrections at the expense of loss of information about the attenuation in the carbon of the scintillator. In practice, data were taken both with and without the gold cover.

Coincidence and anticoincidence cable curves were taken to fix the proper time relationships. The coincidence plateau had a very flat top with sides sloping 7 nsec/decade. Well off the plateau an "accidental" rate between 0.1% and 1% was observed but these events were due to a real proton in B in accidental coincidence with a different proton in A giving the proper fraction of anticoincidences and so not affecting the data. Accidental coincidences, with no proton in B,

TABLE II. Weighted averages over several runs of the attenuation measurements and the various corrections. All entries are in parts per million except where specified.

	Carbon (target)	Carbon (counter)	Mg	Al	Ni	Cu	Pb
E_{lab} (MeV)	16.48	16.28	16.47	16.29	16.33	16.37	16.31
Target thickness (mg/cm²)	23.72±0.06	···	26.9±0.3	43.6±0.2	47.6±0.5	42.9±0.4	70.8±0.7
Raw attenuation	862 ±14	540±50	702 ±9	816 ±10	523 ±9	516 ±9	521 ±9
Elastic scattering	−419 ±15	−30±30	−93 ±5	−140 ±8	−54 ±2	−46 ±2	−174 ±21
Inelastic scattering	+27 ±8	···	+53 ±16	+49 ±20	+45 ±10	+25 ±8	+7 ±7
"C" energy shift	−118 ±11	···	−179 ±16	−10 ±0	−54 ±11	−99 ±11	−57 ±11
Count rate	−14 ±9	−39±13	−46 ±23	−46 ±23	−34 ±16	−34 ±17	−44 ±22
B energy shift	+6 ±5	+12±6	+11 ±6	+11 ±6	+11 ±6	+11 ±6	+13 ±6
C discriminator	+40 ±8	+24±6	+21 ±15	+2 ±0	+7 ±6	+11 ±8	+19 ±7
C backscatter	−6 ±2	···	−9 ±4	−9 ±4	−9 ±4	−9 ±4	−11 ±5
Net attenuation	417 ±33	507±58	473 ±38	683 ±34	439 ±26	385 ±26	274 ±36
σ_R (mb)	382 ±32	348±39	712 ±56	701 ±34	898 ±53	955 ±64	1330 ±180

which would add to the attenuation background and depend on the duty cycle and counting rate, were of the order of a few ppm under normal conditions. The valley in the anticoincidence cable curve had a flat bottom with a gentle slope from the cable attenuation shifting the C discriminator position. The sides of the valley closed in slightly at high counting rates. Outside the valley the ratio $AB\bar{C}/AB$ rose to 100% as expected.

Pulse waveforms could be monitored at key points during the experiment but the great stability of the critical circuitry meant that the need for adjustment was rare.

III. DATA AND ANALYSIS

(a) Target Properties

Foil targets of a few thousandths of an inch thickness were selected to give energy losses between 0.6 and 1.0 MeV. The average thickness was determined by weighing. A dial indicator set up as thickness gauge showed that gradual variations in thickness of no more than 1–2% were present in all targets. In addition the energy lost by the beam in passing each foil was measured in position relative to Al and found to agree with the expected values within 2%. The reaction-cross-section measurement is insensitive to target purity except for heavy impurities in light targets. The attenuation of 20-keV x rays was used to confirm the purity of the Mg and Al targets. A duplicate of the Al target was used as dummy absorber when finding the energy dependence of the attenuation background.

(b) Proton Energy

For direct comparison with the elastic scattering data of Dayton and Schrank[2] a center-of-mass energy of 17.00 MeV at the target center would be desirable. The switching magnet and spectrometer magnet could not reach the necessary momentum and as a constant laboratory energy was simpler to use, the laboratory energy incident on the target was set near 17 MeV with small variations from one run to the next. The energy at the target center then depended on the target energy loss.

A limp wire calibration of the spectrometer in the spring of 1963 with an absolute accuracy of ±50 keV showed an error of 1% in the previous calibration so that the average laboratory energy at the target center was actually about 16.4 MeV and is given precisely for each target in Table II.

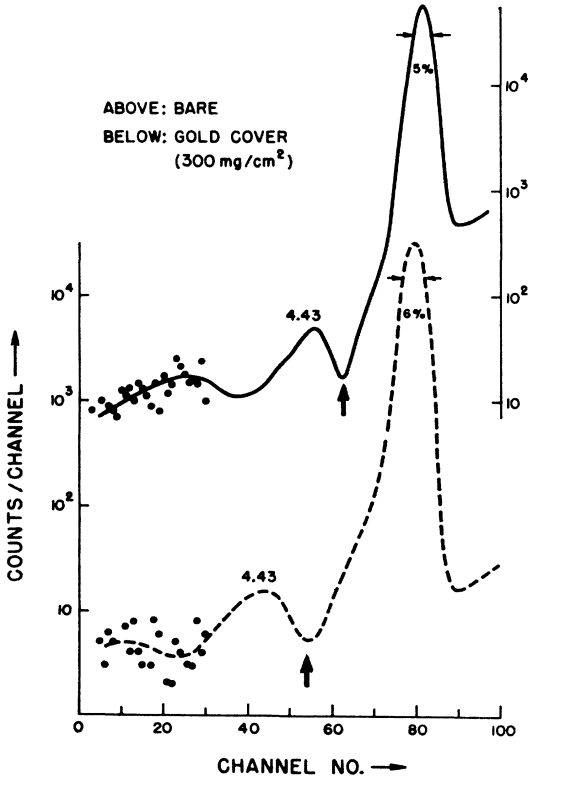

FIG. 6. Spectra from scintillation counter C taken with and without the 300-mg/cm² gold cover in position. Note the logarithmic intensity scale. The secondary peak is given by reactions with C^{12} in the plastic scintillator.

(c) Data Accumulation

Five targets and a blank spare were positioned in the target wheel. Each of these was exposed in turn to a beam of 3000 to 10 000 protons/sec for about 20 min. While the blank position was exposed the dummy absorber before the magnetic spectrometer was inserted and the magnet current lowered to bring the lower energy beam onto the final counter. As the dummy absorber lowered the counting rate at the target, measurements were made at a variety of rates to measure the rate dependence. Various changes in geometry and other factors were made during some twenty days of machine time. Attenuation data from eight days for which a complete set of data was taken is shown in Table II. The four major and three minor corrections shown in the table and discussed in Sec. IV varied with the changes in experimental conditions and were applied separately before determining the over-all error for each target on each day. The error was then used as a weighting factor in the averages shown in the table. The statistical errors are reduced by averaging over many determinations whereas the systematic parts of the correction errors are not, so these tend to dominate the final error quoted for each target. On the four days in which the C scintillator had no gold cover a Pb target was in use and the carbon reaction cross section was found in the Burge[16] method from the energy dependence of the attenuation background using the range-energy relation of Rich and Madey[22] for CH. When the gold cover was added to improve the statistics, the Pb target was replaced by a sheet of the plastic scintillator so that a separate determination for carbon could be made.

(d) Consistency

Two points should be made regarding the quality of the data. If a histogram of the deviations of the individual measured attenuations from the average for each target is plotted, more than 90% of the points form a Gaussian distribution with the width to be expected from the statistical uncertainties. An occasional point lies more than three standard deviations from the mean for which no experimental malfunction was apparent. An unobserved change of gain or energy during a cycle of measurements could have such an effect. Sufficient repetitions of the experiment make the effect of any one such anomalous measurement on the quoted averages small. The second point regards the use of several targets in rapid succession. Because this method was employed the cross sections are tied one to the other with somewhat greater precision than that with which the absolute value of any one is established. Thus, if some unforseen systematic error is present which makes all the values too low, for example, the effect on each target may be deduced. In order to raise the Al value by 50 mb, one would have to accept a rise for Mg of 75 mb, for Ni of 100 mb, for Cu of 125 mb, and for Pb of 240 mb. Thus, too, the difference between the Ni and Cu values is statistically significant even though smaller than the errors quoted for either nucleus separately. Taking into account only the relative errors the difference between the value of σ_R for Cu and Ni is 57 ± 47 mb while the Mg-Al difference is 11 ± 38 mb.

[22] M. Rich and R. Madey, University of California Radiation Laboratory Report No. UCRL 2301, 1954 (unpublished).

IV. CORRECTIONS

The increase in the attenuation ratio $AB\bar{C}/AB$ observed on replacing the dummy absorber with the target proper is caused for the most part by reactions in the target. All other processes which give rise to a changed attenuation during the substitution procedure must be accounted for by an appropriate correction. Seven correction terms have been used in the data reduction and are discussed in turn below.

A single dummy absorber provides the reference for all five targets. As each target foil has a different energy loss, the condition that the beam energy at the final counter is the same for each target as for the dummy is not exactly satisfied. Both the positioning of the discriminator on the "C" counter spectrum and the energy dependence of the attenuation in the "C" counter must be considered.

(a) C Discriminator Positioning

During each run the final counter discriminator was set by visual comparison between gated and ungated spectra to lie at the position marked with an arrow in Fig. 6, 3.3 MeV below the peak. Once this had been done for a single target, the small changes needed to maintain the 3.3-MeV setting for each of the other targets were made using a measured functional relation between proton energy and discriminator position. If this setting method had been perfectly applied during each run, the correction in Table II would be zero. When a more elaborate method of deducing the influence of small deviations from linearity in the photomultiplier and preamplifier was devised, all earlier data were corrected to the improved discriminator positioning. The correction makes use of the fractional area per unit energy at the valley position in the "C" spectrum, averaged over many recorded spectra. The error comes from uncertainty in the valley depth as well as uncertainty in the positioning shift. The correction increases as the difference between target and dummy absorber energy losses increases.

(b) "C" Energy Shift

Setting the discriminator at a standard excitation energy for each target does not make the attenuation background in the C counter the same for each target

because the higher range protons leaving a thin target have a chance to react with more scintillator nuclei. The energy dependence of the C counter background was measured with no target in place by comparing the attenuation measured with and without the dummy absorber. Assuming a fairly smooth dependence on energy of the cross sections in the scintillator, one could then interpolate to the much smaller energy differences between the dummy and the various targets. In essence this correction shifts the attenuation background, measured with the dummy, up to the value it would have had if the dummy had given as small an energy loss as the target. The correction is large where there was a large energy difference between target and dummy, but is as accurately known as the statistics in the counter method of measuring σ_R for carbon.

(c) Counting Rate

Whenever the dummy absorber was inserted, multiple scattering outside the spectrometer-magnet acceptance angle lowered the counting rate at the final C counter. Rate-dependent gain in the C photomultiplier or associated circuitry, by shifting the discriminator level, would then change the attenuation background so that correction to a common counting rate is required before comparing dummy and target measurements. The rate-dependent gain shift could be easily and accurately measured by placing the C discriminator in the middle of the main peak in the C spectrum and observing $AB\overline{C}/AB$ as the rate was varied. The gain shift was linear and reversible in the range of counting rate employed for the experiment but exhibited long-lived shifts or effective hysteresis at rates above 15×10^3 counts/sec. With the measured gain shift and a knowledge of the spectrum shape at the discriminator level, the effect of counting rate on the attenuation background could be deduced.

Direct measurement of the attenuation background at various counting rates was also used but the rate effects were small and could easily be affected by minute gain drifts during a series of measurements. The average of all such direct measurements gave a somewhat larger counting rate correction than the measured gain shift would allow, with poorer precision and a certain lack of reproducibility. Since contributions to the counting rate dependence other than the gain shift of the C counter could not be ruled out completely, the directly measured correction was used, giving the largest source of error in the data of Table II. A consistent policy of alternating high- and low-rate measurements of attenuation would allow a substantial reduction in the error in this correction. All the data were corrected to a common rate rather than to zero rate. This procedure could introduce a systematic error if the rate dependence with the dummy in place were different from the rate dependence with the targets in place, for example from an effect of counting rate on the A counter. The precision of the direct rate-dependence measurements was not sufficient to rule out this possibility completely.

(d) B Counter Attenuation Shift with Energy

When the target was removed and the dummy inserted, the proton energy at counter B was lowered by 1 MeV. Reactions and scattering by the B scintillator and light tight wrapping, which removed particles after causing a count contributed to the attenuation background and the energy dependence of these processes changed the background and required a correction. The computation was complicated by the several changes in B geometry and also by the differential discriminator on this counter. The influence of the latter is manifest for elastic scatter near 90° lab where the long flight path in the scintillator raised the pulse height enough to reject the event and thus not influence the experiment. The B scintillator hydrogen scattering was made negligible by this process and the carbon scattering somewhat reduced, less than for hydrogen because of the insensitivity of plastic scintillator to heavily ionizing recoils. The carbon reaction cross section was assumed constant with energy in this region while the elastic-scattering shift with energy was deduced from the work of Peelle[23] and Daehnick.[3] The aluminum cover was too thin to contribute. The shift in attenuation per MeV was small and ranged from 3 to 15 ppm for the various geometries.

The beam spot at the B counter was about 9 mm wide by 1 mm high so the elastic scatter in B which missed C was higher for the spot edges. The spot was widened slightly by the energy loss straggling in the dummy but the effect, simulated by moving the spot with the magnet current from side to side, was small and could be neglected.

(e) Target Elastic Scattering

Elastic scattering through angles large enough to miss the C counter would cause an attenuation event without a reaction. The elastic correction is found by graphical integration of absolute differential cross sections between limits set by the experimental geometry. The forward limit is the angle subtended by the C counter except when the gold foil cover was in use. The cover thickness increased for slant paths so the discriminator set the effective forward angle. Fixing the limiting angle in the latter way improved the accuracy of the elastic correction; for when the counter was bare, an averaging over the beam spot and scintillator shape was required. In either case the effect of multiple scattering was included to first order. The backward limit of integration was not 180°, for elastic scattering back through counter B would trigger the upper discriminator and reject the event. Differential cross

[23] R. W. Peelle, Phys. Rev. **105**, 1311 (1957).

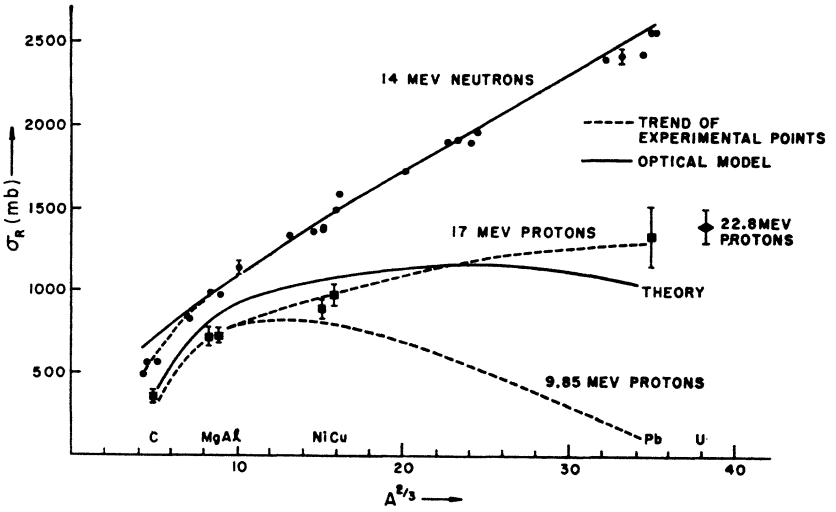

FIG. 7. Experimenta results plotted against $A^{2/3}$ for comparison with other experiments and the predictions of the optical model. The dashed line joining the experimental points does not imply that the intervening values will follow so smooth a behavior.

sections at adjacent energies were available[2–4,23,24] and very slight extrapolations to the proper energy could be made with some confidence. The hydrogen in a plastic target gives substantial elastic scattering. Care must be taken not to count this scattering twice over as the recoils are included in the published elastic cross sections. The correction is converted from a cross section to the equivalent attenuation so as to allow a consistent error treatment in arriving at the weighted averages of Table II.

(f) Target Inelastic Scattering

Forward scattering from states of excitation less than 3.3 MeV was a form of reaction event not registering as an attenuation. The limit of integration was set in the same way as for the elastic correction. The discriminator set an angular limit differing for each state where the cover foil was employed. Inelastic scattering backward through the B counter rejected valid reaction events, and for targets such as Ni with a large evaporation continuum the backward correction was larger than the forward correction. The necessary inelastic differential cross sections were available for some targets, often from unpublished data taken at this laboratory; in other cases the appropriate scattering experiment was performed or the magnitude of the cross section was inferred[12] from neighboring nuclei or data at other energies where available.

(g) Backscatter from the C Counter

Events in the stopping scintillator reducing the pulse height below the discrimination level contribute to the attenuation background. Most such events are reactions. However, some 10% of these events arise from elastic backscattering in which the proton leaves the scintillator before coming to rest. The backscattering contribution to the attenuation background is energy dependent in a complicated way and requires knowledge of elastic angular distributions over a considerable band of energies for proper evaluation. In extracting reaction cross sections for the scintillator nuclei from a measured energy dependence of the attenuation background, the evaluation of the backscattering replaces the simpler elastic correction of the target method.

Scintillator backscattering from the C counter affects the target attenuation measurements to a small extent because a fraction of the protons scatter back through the B counter and reject the event altogether. The fraction is different when the target is interposed between the B and C counters. Both elastic and inelastic backscattering must be considered in the correction which is, however, very small.

V. DISCUSSION

In Fig. 7, the proton total reaction cross sections at 16.4 MeV are plotted against $A^{2/3}$. Reaction cross sections for neutrons[25] of 14.2 MeV and the trend of the 10-MeV proton data[26] are shown for comparison. The curve labeled "theory" indicates the general behavior of the predictions arising from various optical-model analyses of elastic scattering.[7,8,10]

The Coulomb potential is seen to reduce the proton reaction cross sections of the heaviest nuclei by factors of 2 and 10 for proton energies of 20 and 10 MeV, respectively. Reaction cross sections are affected most by the barrier shape where the change of σ_R with energy is most rapid. Since the Coulomb potential is rather well known, σ_R for Pb at 16.4 MeV may be sensitive to surface structure, i.e., to the shape of the tail of the nuclear or Coulomb potential. All the optical predictions

[24] I. E. Dayton, Phys. Rev. **95**, 754 (1954).

[25] M. H. MacGregor, W. P. Ball, and R. Booth, Phys. Rev. **108**, 726 (1957).

[26] B. D. Wilkins and G. Igo, Phys. Rev. **129**, 2198 (1963).

are lower than the measured value by one or two standard deviations.

The usefulness of σ_R measurements in the choice of optical-potential parameters has been examined by Melkanoff *et al.*[1] for Cu at 17 MeV. A measurement of σ_R for Cu with error less than 20 mb would determine the relative amounts of surface and volume absorption in a set of potentials of equal value in describing elastic scattering. The present measurements have not reached the necessary precision for an unambiguous determination, but the low σ_R would appear to favor little or no volume absorption.[27] One must keep in mind, however, that the presence of compound elastic scattering could raise the optical-model prediction relative to the measured σ_R.

The value of σ_R for Ni is significantly less than for Cu in the present measurements and also in the neutron data and the data for 10-MeV protons. The small value for Ni has been attributed by Wilkins and Igo[26] to a smaller radius for that nucleus. However, at least some of the difference may arise from the depth of the real potential. As Perey[10] points out, both a nuclear symmetry term $(N\text{-}Z)/A$ and a Coulomb parameter $Z/A^{1/3}$ influence the depths of the real potential and give rise to a predicted difference in σ_R between Cu and Ni at 17 MeV of about 30 mb if the same radii are used and about 60 mb if the radii giving best fits are used: $r(\mathrm{Ni})<r(\mathrm{Cu})$. The measured difference is consistent with either of these predicted differences even though the absolute values of the predicted σ_R for Ni and Cu are too large by about 80 mb.

Neutron yields from proton bombardment of thick targets[28] show pronounced minima at $Z=28$ and at $Z=39$. Perhaps one should be suprised that σ_R for Ni can remain as large as it is, with this normally most prolific reaction strongly inhibited. The reaction which is enhanced to compensate for the neutron inhibition in Ni^{58} is inelastic proton scattering to the continuum. The compound elastic scattering cannot be larger in Ni than in Cu by more than a few tens of millibarns without disturbing the agreement mentioned in the preceding paragraph. The neutron yield measurements suggest that a second dip in σ_R may be expected near Zr.

The two nearly independent determinations of σ_R for carbon agree well within the experimental errors. An incorrect assessment of the H elastic scattering from the plastic target gave rise to a discrepancy in earlier reports of these measurements.[12] A third determination by summation of the partial cross sections for all reactions possible at the given energy is again in very good agreement giving considerable indirect support for the absence of systematic errors in the σ_R values for the other nuclei. The work on carbon which has been extended over a wide range of energies will be reported separately in greater detail. Data on separate reactions for the heavier nuclei is insufficiently accurate to let the summation method compete with the attenuation measurements.

To summarize, proton total reaction cross sections, measured at a laboratory energy of 16.4 MeV for targets of C, Mg, Al, Ni, Cu, and Pb, are reasonably consistent with the values expected from the trend of other data and with predictions of the optical model. Differences in detail are apparent, however, notably a measured value for Pb larger and values for Cu and Ni somewhat smaller than expected from optical-model predictions based on fits to elastic scattering alone. Systematic errors, if present, would have to raise or lower all measurements together and are bounded by the agreement of three independent methods for carbon so the small disagreements with the present optical-model predictions are probably genuine. Attenuation measurements of σ_R with 5 to 10% accuracy appear then to be useful although the real value will come from second-generation experiments in the 2% accuracy range.

ACKNOWLEDGMENTS

The authors are indebted to Professor R. Sherr for valuable suggestions and a great deal of encouragement during the course of the experiment and to many members of the Princeton cyclotron group for the use of unpublished data in some of the corrections.

[27] See however, J. Olkowski, M. A. Melkanoff, and J. S. Nodvik, in *Proceedings of the Conference on Direct Interactions and Nuclear Reaction Mechanisms, Padua, 1962*, edited by E. Clementel and C. Villi (Gordon and Breach Publishers, Inc., New York, 1963), p. 193.

[28] Y. Tai, G. P. Millburn, S. N. Kaplan, and B. J. Moyer, Phys. Rev. **109**, 2086 (1958).